IEEE Sensors Council

A Multiple Mobile Chargers Collaboratative Recharging Scheme for Enhanced Data Quailty and Sustainable Lifetime in WRSNs

Zhijie Hu, Xiaolin Gui, *Member, IEEE*, Chih-Yung Chang, *Member, IEEE*, Xu Zhang, and Diptendu Sinha Roy

***Abstract*—With the rapid advancement of Internet of Things (IoT) technology, wireless sensor networks (WSNs) have become increasingly pivotal across various domains. However, the limited battery life of sensor nodes remains a critical bottleneck affecting their development and sustainability. In wireless rechargeable sensor networks (WRSNs), existing multiple mobile chargers (MCs) approach face challenges, including uneven node distribution, suboptimal charging station placement, and poor coordination, resulting in diminished recharging efficiency and degraded surveillance quality. Therefore, this study proposes a cooperative recharging mechanism for WRSNs based on multiple MCs. This mechanism first uses attractive-repulsive forces and Voronoi diagrams to achieve sensor relocation, resulting in a more balanced distribution of sensor nodes and improved spatial surveillance quality. Second, by optimizing the number and location of recharging stations (RSs) and dividing the surveillance area into multiple subregions, each served by a single MC, recharging efficiency is enhanced while satisfying the energy capacity constraints of MCs. Finally, the batch recharging strategy is adopted, and the sensing frequency of sensors are adjusted based on the recharging interval to improve temporal surveillance quality. Simulation results demonstrate that the proposed mechanism outperforms existing algorithms in terms of energy consumption, recharging efficiency, and surveillance quality, effectively extending the lifetime of WRSNs and improving surveillance quality, providing a new perspective for the sustainable development and application of WRSNs.**

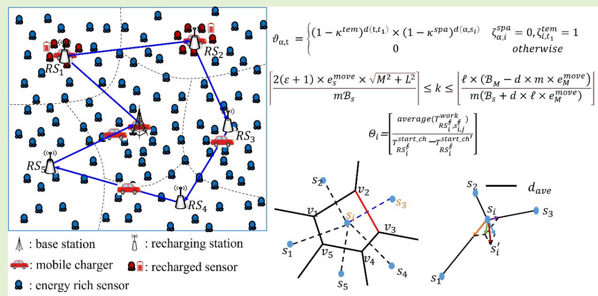

***Index Terms*— Batch recharging, cooperative recharging, mobile charger (MC), wireless rechargeable sensor networks (WRSNs).**

Received 21 April 2025; revised 14 July 2025; accepted 14 July 2025. Date of publication 25 July 2025; date of current version 3 September 2025. This work was supported in part by the National Key Research and Development Program under Project 2022YFB3305502 and Project 2022YFB3305503 and in part by Shaanxi Natural Science Foundation Key Project under Grant 2023-JC-ZD-38. The associate editor coordinating the review of this article and approving it for publication was Prof. Yongqiang Zhao. *(Corresponding author: Chih-Yung Chang.)*

Zhijie Hu is with the Department of Computer Science and Technology, Xi'an Jiaotong University, Xi'an 710000, China, and also with the School of Information Engineering, Xi'an Eurasia University, Xi'an 710000, China (e-mail: huzhijie@eurasia.edu).

Xiaolin Gui is with the Department of Computer Science and Technology, Xi'an Jiaotong University, Xi'an 710000, China (e-mail: Xlgui@mail.xjtu.edu.cn).

Chih-Yung Chang is with the Department of Computer Science and Information Engineering, Tamkang University, New Taipei 25137, Taiwan (e-mail: cychang@mail.tku.edu.tw).

Xu Zhang is with the Department of Computer Science and Technology, Xi'an Jiaotong University, Xi'an 710000, China, and also with Gansu Tongxing Intelligent Technology Development Company Ltd., Lanzhou 730000, China (e-mail: 24093352@qq.com).

Diptendu Sinha Roy is with the Department of Computer Science and Engineering, National Institute of Technology Meghalaya, Shillong 793003, India (e-mail: diptendu.sr@nitm.ac.in).

Digital Object Identifier 10.1109/JSEN.2025.3590479

NOMENCLATURE

L	Length of the monitoring region.
W	Width of the monitoring region.
S	Set of n sensors deployed in the monitoring region, $S = \{s_1, s_2, \ldots, s_n\}$.
e_M^{ch}	Recharging rate of the mobile charger.
e_M^{move}	Moving discharging rate of the mobile charger.
v_M	Moving speed of the mobile charger.
$\mathcal{B}_M$	Battery capacity of the mobile charger.
$\mathcal{B}_s$	Battery capacity of each sensor.
v_s	Moving speed of each mobile sensor.
e_s^{move}	Moving discharging rate of the sensor.
e_i^{work}	Energy discharging rate of the sensor s_i for working.
f_i	Sensing frequency of the sensor s_i.
r_s	Monitoring radius of the sensor s_i.
$\vartheta_{\alpha,t}$	Spatial and temporal surveillance quality of the point α at time t.
V_i	Voronoi cell of sensor s_i.
$\mathcal{G}_{s_i}$	Areas of the V_i.

k	Number of the RSs in each subregion.
ρ	Density of the RSs.
d	Average distance between the two adjacent RSs.
m	Number of the subregions.
ℓ	Recharging efficiency rate of the mobile charger.
RS_i^{ℓ}	ℓth RS of the ith subregion.
S_i^1	Set of sensors in the cluster of RS_i^1, $S_i^1 = \{s_{i,1}^1, s_{i,2}^1, \ldots, s_{i,u}^1\}$.
$l_{s_{i,j}^1}$	Location of the sensor $s_{i,j}^1$.
$\mathcal{B}^{\text{move}}_{\mathrm{RS}_i^1, s_{i,j}^1}$	Energy consumption of the sensor $s_{i,j}^1$ for moving from $s_{i,j}^1$ to RS_i^1.
$\mathcal{B}^{\text{rem}}_{\mathrm{RS}_i^1, s_{i,j}^1}$	Remaining energy of the sensor $s_{i,j}^1$ for executing monitoring work.
$T^{\text{rech}}_{\mathrm{RS}_i^1, s_{i,j}^1}$	Time period required for the sensor $s_{i,j}^1$ being recharged by the mobile charger.
$T^{\text{start\_ch}}_{\mathrm{RS}_i^1}$	Starting recharging time of the RS_i^1.
C	Set of $m \times k$ clusters, $C = \{c_1, c_2, \ldots, c_{m\times k}\}$.
Θ_i	Number of batches of the sensors in the c_i.
f_i^{new}	Adjusted working frequency of the s_i.

I. Introduction

Wireless sensor networks (WSNs) are widely used in fields such as smart farming [1], smart grid [2], industrial control [3], and human health monitoring [4]. However, the limited battery life of sensor nodes has constrained their broader development. Recent advancements in wireless energy transfer technologies [5], e.g., magnetic resonant coupling [6], have enabled mobile chargers (MCs) to wirelessly recharge sensor nodes, thereby extending network lifetime [7], [8], [9].

Current research on energy replenishment for WSNs primarily categorizes methods into single-MC recharging and multi-MC recharging. Single-MC charging includes periodic recharging and on-demand recharging [10], [11]. In periodic recharging, the MC follows a fixed route and schedule [12], often causing uneven energy distribution. Some nodes may be overcharged while others face energy depletion, compromising monitoring quality. To address this issue, some researchers have focused on developing on-demand charging methods.

In on-demand charging, the MC schedules recharging based on the sensor's recharging needs, the importance of the monitoring tasks, and the distance from the MC, while optimizing MC recharging paths to minimize time and energy. However, dense node distributions often overwhelm single MC, prompting multi-MC solutions.

Multi-MCs schemes partition the monitoring area into subregions serviced by individual MCs. However, random node distribution creates uneven workloads: dense regions overwhelm MC capacity while sparse regions underuse them. Current approaches also lack MC coordination, causing recharge delays that may disrupt network operations.

To address these challenges, this study proposes a cooperative recharging scheme for wireless rechargeable sensor networks (WRSNs) using multiple MCs. This study not only ensures the perpetual lifetime of sensor nodes but also maintains high surveillance quality, including both spatial and temporal monitoring performance.

The main contributions of the proposed algorithm are as follows.

1) *Maximizing Space Surveillance Quality:* This study addresses the common issue of uneven sensor distribution by introducing a sensor relocation algorithm based on attractive-repulsive forces and Voronoi diagrams. This algorithm achieves a more balanced distribution of sensor nodes, which leads to improved spatial data quality across the monitoring region.
2) *Enhancing Temporal Surveillance Quality:* To minimize energy consumption during MCs' movement for recharging sensors, the algorithm assumes sensor mobility. At the starting recharging time, sensors arrive at recharging stations (RSs) to be recharged by the MCs. This implies that sensors are unable to perform monitoring tasks during the recharging process, leading to lower monitoring quality. To solve this issue, this study proposes a batch recharging mechanism that optimizes the recharging schedule. In addition, the proposed algorithm adjusts the monitoring frequency of sensors based on the starting recharging time and their power consumption rates, aiming to improve the temporal monitoring quality.
3) *Improving the Recharging Efficiency:* The proposed algorithm determines the placement and number of RSs, aiming at minimizing the energy consumption of MCs and reducing the travel distance required for both MCs and sensors. The proposed algorithm considers the constraints of MCs' energy capacity and the operational efficiency of sensors, resulting in a more efficient recharging process.

The remainder of this article is organized as follows. Section II reviews related prior research. Section III formulates the network model, energy model, and monitoring model. Section IV describes the algorithmic approach. Section V analyzes the simulation results. Finally, Section VI summarizes this article and outlines directions for future work.

II. Related Works

This section describes the research related to recharging in WRSNs based on a mobile recharger. These studies are mainly divided into single MC and multiple MC technologies.

A. Single MC Technologies

The charging methods for a single MC can be categorized into periodic charging and on-demand charging. In periodic charging technology, the path of MC is preplanned based on network information. During the recharging process, the recharging route and sequence do not change. The MC provides periodic recharging to the sensors along the route at fixed intervals.

Liu et al. [13] proposed an active charging scheme in which the MC dynamically moved toward clusters of sensor nodes, aiming to prolong the lifetime of the network. The algorithm began by estimating the energy consumption of nodes serving as cluster heads, which is crucial for determining the optimal charging strategy. Let $\mathcal{R}_p^{[H]}$ represent the expected energy consumption of a cluster head node. Let $\mathbb{E}(d_H)$ denote the expected maximum multihop distance. Let ρ denote the node density. Let e_r and e_t represent the energy consumptions for data reception and transmission, respectively. Let e_s denote the energy consumption for data sensing. Let λ denote the average number of data packets generated per unit time, and τ denote the duration of one service cycle. The value of $\mathcal{R}_p^{[H]}$ can be calculated by the following equation:

$$\mathcal{R}_p^{[H]} = \left[\pi \mathbb{E}(d_H)^2 \rho(e_r + e_t) + (e_s + e_t)\right]\lambda\tau. \tag{1}$$

Based on this estimation, each sensor node autonomously decided whether to act as a cluster head by comparing its residual energy with the estimated energy consumption of a cluster head. Nodes with residual energy close to the estimated value were more likely to be selected as cluster heads, ensuring that energy-hungry nodes received timely charging. During the charging process, the MC only visited cluster head nodes and other sensors with low residual energy, reducing the number of nodes that needed to be charged and thereby shortening the charging path. Experimental results demonstrated that the proposed scheme significantly reduced the charging path length and improved the energy efficiency of the network.

Wei et al. [14] proposed an energy replenishment and data collection strategy in WRSNs. The MC was used to collect data acquired by sensors while charging the sensor nodes. This dual functionality of the MC implied that its path planning significantly impacted both the lifespan of the sensors and the efficiency of data collection. To address this, the authors formulated a multiobjective optimization model aimed at maximizing the energy usage efficiency of the MC while minimizing the average delay of data transmission. Let ϕ denote the energy usage efficiency of the MC. Let E_{cons}^r denote the energy consumption of the rth charging round ($r = \{1, 2, \ldots, R\}$). Let $E_{\text{tra}}^{\max}$ and $E_{\text{ch}}^{\max}$ represent the maximum traveling energy and the maximum charging energy of the MC, respectively. The value of ϕ was calculated by the following equation:

$$\phi = \frac{\sum_{r=1}^{R} E_{\text{cons}}^r}{R\left(E_{\text{tra}}^{\max} + E_{\text{ch}}^{\max}\right)}. \tag{2}$$

Let $\overline{\Delta\tau}$ denote the average data transmission delay. Let N represent the number of sensor nodes. Let t_i denote the time when the MC arrives at sensor s_i. Let t_i^q represent the data transmission request time of the s_i. The value of $\overline{\Delta\tau}$ can be obtained using the following equation:

$$\overline{\Delta\tau} = \frac{1}{N}\sum_{i=1}^{N}\left(t_i - t_i^q\right). \tag{3}$$

This approach ensured that the MC not only extended the network's operational lifetime by efficiently replenishing energy but also enhanced the overall data collection performance by reducing transmission delays.

The periodic charging algorithms adopted in [13] and [14] are suitable for networks where sensors are uniformly distributed and have the same energy consumption rate. If different sensors have varying power consumption, the MC needs to dynamically adjust its path and charging sequence based on the sensors' requirements. Therefore, the methods proposed in studies [13] and [14] are not applicable.

Unlike periodic charging, the recharging path of the MC and the recharging sequence of sensors in on-demand charging algorithms are variable. Nguyen et al. [15] proposed an on-demand charging scheduling method that combined fuzzy logic and Q-learning to maximize the lifetime of WRSNs. The algorithm employed Q-learning to determine the optimal charging sequence of sensors. The Q-learning framework was designed to prioritize sensors based on their contribution to target monitoring and network connectivity. The Q value for each charging location was updated using the following equation:

$$\begin{aligned} Q(D_c, D_i) \leftarrow\ & Q(D_c, D_i) + \alpha(r(D_i)) \\ & + \gamma \max_{1\le j\le l} Q\left(D_i, D_j\right) - Q(D_c, D_i) \end{aligned} \tag{4}$$

where $Q(D_c, D_i)$ represented the Q value for moving from the current charging location D_c to the next location D_i, α is the learning rate, $r(D_i)$ is the reward function that evaluates the effectiveness of charging at location D_i, and γ is the discount factor.

In addition, the algorithm used fuzzy logic to dynamically determine the optimal charging time at each charging location. The fuzzy logic algorithm considered multiple input parameters, including the sensors' remaining energy, energy consumption rate, and distance to the charging location. Let E_{sf} denote the safe energy level. Let E_{th} represent the energy threshold for sending a charging request, and $E_{\max}$ represent the maximum energy capacity of the sensors. Let θ denote the safe energy factor determined by the fuzzy logic algorithm. The value of the E_{sf} can be calculated by the following equation:

$$E_{\text{sf}} = E_{\text{th}} + \theta E_{\max}. \tag{5}$$

By combining Q-learning and fuzzy logic, the algorithm dynamically adjusted the charging sequence and charging time, ensuring that critical sensors were recharged in time to maintain target coverage and network connectivity.

Dande et al. [16] proposed a coverage-aware recharging scheduling algorithm for WSNs that, similar to [15], considered the varying contributions of different sensors in terms of coverage and energy consumption. The proposed algorithm was divided into three phases: Initialization, recharging scheduling, and path construction. During the recharging scheduling phase, the algorithm prioritized sensors based on their coverage contribution and path cost. Two algorithms were proposed: the cost-effective (CE) algorithm, which selected sensors with the lowest remaining energy and determined optimal recharging times to maximize survival; The CE with considerations of coverage and fairness (C^2F) algorithm, which additionally accounts for the chain effect of recharging, balancing coverage loss and the benefits of each candidate charging location. Let $\varnothing_{x,y}^{\text{benefit}}$ denote the benefit of recharging at the grid $g_{x,y}$. Let E_i^{crg} represent the energy recharged to sensor s_i. Let c_i^{sen} denote the coverage contribution of s_i. Let $S_{x,y}^{\text{rcg}}$ denote the set of sensors whose recharging ranges encompass the grid $g_{x,y}$. Equation (6) calculated the value of $\emptyset_{x,y}^{\text{benefit}}$

$$\emptyset_{x,y}^{\text{benefit}} = \frac{\sum_{s_i \in S_{x,y}^{\text{rcg}}} E_i^{\text{crg}} \times \bigcup_{s_i \in S_{x,y}^{\text{rcg}}} c_i^{\text{sen}}}{\left|S_{x,y}^{\text{rcg}}\right|}. \tag{6}$$

Let $\emptyset_{x,y}^{\text{weight}}$ represent the weight of grid $g_{x,y}$. Let $d(l_a, l_b)$ denote the distance from the current position l_a of the MC to the position l_b of the target grid $g_{x,y}$. The value of $\emptyset_{x,y}^{\text{weight}}$ can be calculated by the following equation:

$$\emptyset_{x,y}^{\text{weight}} = \frac{\emptyset_{x,y}^{\text{benefit}}}{d(l_a, l_b)}. \tag{7}$$

Based on the scheduling results, the MC constructed a recharging path that passed through the top-k grids with the highest weights. The path was designed to maximize the monitoring quality of the entire surveillance area while minimizing the energy consumption of the MC.

Both [15] and [16] adopted the on-demand recharging method using a single MC, which was suitable for small-scale WSNs. Because of the limited battery capacity, the MC needs to periodically visit RSs to recharge. During this period, the recharging needs of sensors cannot be met, leading to sensors running out of power and being unable to perform monitoring tasks. Furthermore, in large-scale WRSNs, the number of sensors is significant, rendering a single MC insufficient to fulfill the recharging tasks.

B. Multiple MC Technologies

Yadav and Dash [17] proposed an anchor-based algorithm for multi-MCs recharging and data collection. The algorithm is based on the assumption that m circles of radius p cover all sensors in the monitoring area, with the centers of these circles located at the anchor points. The anchor points were then partitioned into k groups, with each MC responsible for the recharging and data collection tasks of one group. The MCs collected the data from the sensors while recharging them. The key objective of the algorithm was to optimize the energy use efficiency and data collection per unit energy. Let EU_{eff}^r denote the energy use efficiency. Let T represent the cycle time. Let τ_j^r denote the sojourn time at anchor point j. Let $\text{ECR}(\text{rs}_{i,j}^r)$ denote the energy consumption rate of sensor $\text{rs}_{i,j}^r$. Let TE_{con}^r represent the total energy consumed by the MC for traveling, data gathering, and charging. The value of EU_{eff}^r can be gained using the following equation:

$$\text{EU}_{\text{eff}}^r = \frac{\sum_{j=1}^{m^r} \sum_{i-1}^{n_j} \left(T - \tau_j^r\right) \times \text{ECR}\left(\text{rs}_{i,j}^r\right)}{\text{TE}_{\text{con}}^r}. \tag{8}$$

This approach significantly reduced the number of anchor points and improved the overall efficiency of the network by minimizing the energy consumption and maximizing the data collection rate.

Dong et al. [18] proposed an instant on-demand charging strategy (IOCS) to maximize the energy efficiency of the MCs and the survival rate of the sensor nodes in WRSNs. The algorithm partitioned the monitoring region into multiple subregions using an improved K-means algorithm, where each MC was responsible for recharging the sensor nodes within its designated subregion. The priority of sensors for charging was determined by integrating multiple factors, including the distance to the MC, remaining battery level, and energy consumption rate. Let H_i denote the temporal-event energy priority of sensor s_i. Let e_i and p_i denote the residual energy and energy consumption rate of s_i. The value of H_i can be calculated using the following equation:

$$H_i = \frac{e_i}{p_i} = 1 - \sqrt[3]{(1 - p_i \cdot t)}. \tag{9}$$

Let $\text{RE}_i^{(j)}$ denote the united charging priority. Let L_i^j represent the spatial energy priority, which reflects the distance between sensor s_i and MC W_j. Equation (10) calculated the value of $\text{RE}_i^{(j)}$

$$\text{RE}_i^{(j)} = \cos\left(\arctan\left(\frac{H_i}{L_i^j}\right)\right). \tag{10}$$

Sensors with higher $\text{RE}_i^{(j)}$ values were prioritized for recharging, ensuring an optimal balance between sensor survival and MC energy efficiency. Both [17] and [18] proposed multi-MCs strategies, but there was no cooperation between the MCs.

Qaisar et al. [19] proposed an ISAC-assisted charging algorithm for WRSNs with multiple MCs. This algorithm optimized charging efficiency through three key strategies: First, the charging queue for each MC was prioritized using a multimetric strategy based on residual energy of the sensor E_{res}, distance between the MC and the sensor d, number of neighbors K_{num}, and betweenness centrality C_{btw}. Let P denote the charging priority metric. The value of P is calculated by the following equation:

$$P = \omega_1 \cdot \hat{E}_{\text{res}} + \omega_2 \cdot \hat{d} + \omega_3 \cdot \hat{K}_{\text{num}} + \omega_4 \cdot \hat{C}_{\text{btw}} \tag{11}$$

where $\hat{}$ denotes normalized values (scaled to [0, 1]) and ω_i are weights reflecting attribute importance. Second, the charging control factor limits the energy transferred to each sensor to 10% of its residual energy threshold, reducing delays and improving coverage. Finally, integrated sensing and communication (ISAC) enables sensors to detect nearby MCVs via matched filtering of echo signals, minimizing travel distance and avoiding charging conflicts. While the algorithm enhanced charging efficiency, it did not address the impact of partial charging on the monitoring quality of the target region.

Cheng et al. [20] addressed the energy replenishment problem in WRSNs with mobile sensors. The study proposed two novel algorithms: an energy balancing algorithm and a redundant sensor dispatch algorithm, both aimed at extending the network lifetime.

The energy balancing algorithm adopted a cascaded movement strategy, where higher-energy sensors replace lower-energy ones to maintain continuous monitoring. This strategy was optimized using (12), which selected sensors based on their effective remaining energy

$$\max\ E = E_r(s_z) - (E_c(s_z, D(s_z, t_k)) + (E_c(s_z, D(t_{k,B})) + \text{MS}) \quad \forall s_z \in S(\text{area}) \tag{12}$$

TABLE I
COMPARISONS OF THE PROPOSED MECHANISM WITH THE RELATED STUDIES

Related work	Periodic single MC	On-demand single MC	Multiple MCs	Cooperation between the MCs	Spatial data quality	Temporal data quality	Sensor mobility	Recharging efficiency
[13]	○	×	×	×	×	×	×	low
[14]	○	×	×	×	×	×	×	low
[15]	×	○	×	×	×	×	×	×
[16]	×	○	×	×	○	×	×	low
[17]	×	×	○	×	○	×	×	low
[18]	×	×	○	×	×	×	×	low
[19]	×	×	○	○	○	×	×	low
[20]	×	×	○	○	○	×	○	low
[21]	×	×	○	○	○	×	○	low
The proposed mechanism	×	×	○	○	○	○	○	high

where notation $E_r(s_z)$ denoted the remaining energy of sensor s_z, notation $E_c(s_z, D(s_z, t_k))$ represented the energy required for sensor s_z to move to the target t_k, notation $E_c(s_z, D(t_{k,B}))$ denoted the energy required for s_z to return to the charging station B after monitoring the target t_k, notation MS represented margin of safety, and notation $S(\text{area})$ denoted the set of sensors located within the specified intersection area. Equation (12) ensured that sensors with the highest effective remaining energy were prioritized for cascaded movement, thereby balancing energy consumption and preventing critical sensor depletion.

The redundant sensor dispatch algorithm replaced depleted sensors with fully charged redundant ones. When redundancy was limited, selection was based on a weight metric computed using (13). Let $W(s_i)$ denote the weight of sensor s_i. Let $E_r(s_i)$ represent the remaining energy of s_i. Let $E_c(s_i, D(s_i, B))$ denote the energy required for s_i to return to the charging station B. This weight-based prioritization ensured that the most energy-depleted sensors were replaced first, thereby preventing network downtime and extending the overall network lifetime

$$W(s_i) = \frac{1}{E_r(s_i) - E_c(s_i, D(s_i, B))}. \tag{13}$$

Hung [21] proposed a mobile sensor-based energy replenishment mechanism for WRSNs. The study introduced a novel approach where certain mobile sensors acted as MCs, replenishing energy for other sensors with insufficient energy to extend the network's lifetime. The algorithm assumed that sensors within the energy transmission area could harvest natural energy sources, such as solar and wind, and convert them into electrical power. These sensors not only replenished their own energy but also transmitted the remaining power to sensors in other areas through wireless energy transmission. Let $E(t)$ denote the residual energy in the environment at t. Let E_{init} represent the initial energy of the sensor network. Let $\overline{EH}_0$ and $\overline{EC}_0$ denote the total amount of energy harvested by sensors in the charging zone and consumed for environment monitoring, respectively. Let $\overline{EC}$ represent the total energy consumed by the sensors due to energy transmission and movement over the time period t. Equation (14) calculated the value of $E(t)$. This article evaluated the energy status of the sensor network through the value of $E(t)$, thereby further optimizing energy management strategies to ensure the sustainability of the network

$$E(t) = E_{\text{init}} + \overline{EH}_0 - \overline{EC} - \overline{EC}_0. \tag{14}$$

Both [20] and [21] allowed sensors to play the role of MCs, which can recharge other sensors or perform monitoring tasks instead of sensors with low energy. The sensors communicated and cooperated with each other. The algorithm not only prolonged the lifetime of the sensor network but also took the monitoring quality into account. However, both [20] and [21] assumed that sensors provided full coverage of the monitored area and that sensors were redundant, which was a too stringent assumption that did not align with practical scenarios.

This study focuses on completing the recharging tasks of WRSNs through the cooperation of multiple MCs, aiming to maximize data surveillance quality while sustaining the lifetime of WRSNs. The proposed algorithm uses repulsive and attractive forces to achieve an even distribution of randomly deployed sensors, ensuring consistency in spatial monitoring quality. The monitoring area is divided into several clusters, and each cluster is equipped with an RS. At the starting recharging time, the sensors move to the RS to be recharged by the MCs. By determining the number and location of RSs, the recharging efficiency of MCs is improved. Table I compares the proposed algorithm with related studies. This study proposes a cooperative recharging approach with multiple MCs, where the MCs recharge the sensors while collecting monitoring data from the sensors. This study reduces the travel energy consumption of MCs through the cooperation between sensors and MCs. While ensuring surveillance quality, it maximizes the number of sensors being charged simultaneously, thereby enhancing the charging efficiency.

The multi-MC's charging mechanism proposed in this study demonstrates significant application potential across various real-world scenarios, including smart agriculture, industrial Internet of Things (IoT), and environmental monitoring systems. For example, in farmland monitoring, sensor networks need to collect data such as soil moisture, temperature, and light for a long time, but frequent battery replacement is costly. This study can charge the sensor on demand through the MCs and dynamically adjust the monitoring frequency to achieve efficient energy management. In industrial equipment monitoring systems, sensors must provide real-time feedback on critical parameters, e.g., mechanical vibration and temperature. The MCs are deployed to inspect the production line, and the sensor data is collected while charging to meet the high real-time requirements. At the same time, the batch charging strategy can reduce the downtime of the production line. In environmental monitoring, sensors can monitor temperature, humidity, and air quality in real time. The MCs can charge the nodes in the monitoring area regularly. The even sensor placement algorithm in this study can adapt to the terrain change and ensure full monitoring coverage without any gaps.

III. Assumptions and Problem Formulation

This section first presents the network environment and energy consumption model. Then, the surveillance quality model, objective, and constraints of this study are introduced.

A. Network Model

This article considers the two-dimensional monitoring region R with size $L \times M$, where L and M are the length and width of R, respectively. In this region, the base station has two roles: recharging the MC and storing the data sensed by sensors. It is assumed that there are n mobile sensors, denoted by $S = \{s_1, s_2, \ldots, s_n\}$, randomly deployed in region R. Assume that all sensors are battery-powered. This study uses the MC to recharge the sensors, aiming to maintain the perpetual lifetime and improve the surveillance quality. There are $m + 1$ MCs in the monitoring region R. The m MCs aim to recharge the sensors on demand, and one MC stays at the base station in a standby state. The energies of all MCs are limited. This article will calculate the number and the locations of the RSs, or RS in short. According to the number of RSs, the whole region will be apportioned into several grids, each of which will be installed an RS. In each grid, the sensors and one MC will move to the RS at the appointed time, and the MC recharges the sensors and collects their sensing data.

The scenario of the considered network is shown in Fig. 1. The monitoring region is divided into six grids. The base station recharges the sensors in the center grid, and the other five MCs are responsible for recharging the sensors in the other five grids. In Fig. 1, the blue line denotes the recharging path of the MCs. The two MCs are recharging the sensors at RS_1 and RS_2 while the other three MCs are moving to the next RS for delivering recharging service.

Section III-B will describe the energy consumption models of the MCs and sensors.

B. Energy Consumption Model

Let $\mathcal{B}_M$ denote the battery capacity of each MC. In each grid, the MC and sensors move to the rendezvous point, denoted by RS, for recharging the sensors. Let v_M denote the speed of each MC. Let e_M^{ch} and e_M^{move} denote the energy consumption for recharging and moving of each MC, respectively. It is noticed that the notations v_M, e_M^{ch} and e_M^{move} are constants.

Let $\mathcal{B}_s$ denote the battery capacity of each sensor. The sensors are mobile and can automatically move to the RS for recharging, reducing the time and energy required for the MC. After recharging, the sensors return to their location to continue sensing. Let v_s denote the movement speed of each sensor. Let e_s^{move} denote the movement consumption of each sensor. Let e_i^{work} and f_i denote the energy discharging rate and the sensing frequency of the sensor s_i, respectively.

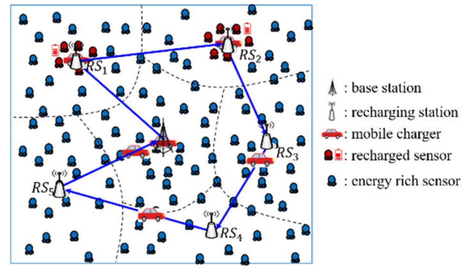

Fig. 1. Scenario of the considered network.

The model for wirelessly recharging sensors via MCs is presented in (15) [7], where G_M, and G_s represent the gains of the MC's antenna and the sensor's antenna, respectively. Let η denote the rectifier efficiency. Let L_p denote the polarization loss, λ denote the wavelength, and d denote the distance between the MC and the sensor. The parameter β is used to adjust the Friis free-space formula for short-distance transmissions. Let P_t and P_r denote the energy transmitted by the MC and the energy received by the sensor, respectively. Equation (15) gives the derivation of P_r

$$P_r = P_t \times \frac{\eta G_M G_s}{L_p} \left(\frac{\lambda}{4\pi (d + \beta)} \right)^2 . \tag{15}$$

The energy consumption of the sensor mainly includes the energy used for recharging traversal, monitoring tasks, and communication with the MCs and the other sensors. Let $\mathcal{B}_s^{\mathrm{move}}$ denote the moving energy consumption of the sensor for being recharged. Let $\mathcal{B}_s^{\mathrm{ford}}$ denote the energy required for moving from the sensor location to the RS. Let $\mathcal{B}_s^{\mathrm{back}}$ denote the energy required for moving from the RS to the sensor location. The value of $\mathcal{B}_s^{\mathrm{move}}$ is obtained by (16). Let $\mathcal{B}_{s,k}^{\mathrm{rece}}$ denote the energy consumption of the sensor to receive k bit. The value of $\mathcal{B}_{s,k}^{\mathrm{rece}}$ is calculated by (17), where the notation $\mathfrak{g}$ denotes the energy expenditure of the receiving circuit per bit. Let $\mathcal{B}_{s,k}^{\mathrm{tran}}$ denote energy consumption of a sensor for transmitting k bits at a distance d. Let $\hbar$ and $\mathscr{w}$ denote the energy consumption per bit for the transmission circuit and the amplification circuit, respectively. Equation (18) depicts the calculation of the notation $\mathcal{B}_{s,k}^{\mathrm{tran}}$

$$\mathcal{B}_s^{\mathrm{move}} = \mathcal{B}_s^{\mathrm{ford}} + \mathcal{B}_s^{\mathrm{back}} \tag{16}$$

$$\mathcal{B}_{s,k}^{\mathrm{rece}} = k \times \mathfrak{g} \tag{17}$$

$$\mathcal{B}_{s,k}^{\mathrm{tran}} = k \times \hbar + k \times d^2 \times \mathscr{w}. \tag{18}$$

Nomenclature lists the main notations in this article.

C. Surveillance Qualities Models

The surveillance quality is determined by the accuracy of the monitoring data collected in region R. The data accuracy refers to the difference between the reported data and the real data. The data accuracy can be measured from two aspects: the spatial and temporal data accuracies. For example, there are several sensors deployed in a monitoring region, aiming to detect the degree of PM2.5. In case the user wants to query the PM2.5 at location a, but there is no sensor at a. Assume that sensor s, which is deployed at location b, is the closest sensor to the query location a. The monitoring system will report the data detected by the sensor s. If the distance between locations a and b is short, the spatial accuracy is high. This is because the reported data and actual data are very close due to the short distance between locations a and b. However, if the distance between a and b is long, the detected data and actual data might have a big difference. In this case, the spatial accuracy is low. Therefore, the spatial accuracy mainly depends on the distance between the user query location and the location of the closest sensor.

Similarly, consider location b. In case the user wants to query the PM2.5 of location b at time t. However, the sensor s does not monitor at time t. Assume the sensor s works at the time t_1 which is the nearest to t. The monitoring system will report the sensed data of time t_1. If the time difference between t and t_1 is small, the temporal accuracy is high. Otherwise, the temporal accuracy is low. This is because the proximity between the reported data and the real data is proportional to the time difference of t and t_1.

The following will present an accuracy measurement model that measures the surveillance quality from spatial and temporal aspects. Let r_s denote the monitoring radius of the sensor s_i. Let $\zeta_{\alpha,i}^{\text{spa}}$ be a Boolean variable, indicating whether or not the point $\alpha \in R$ falls in the sensing range of sensor s_i. If α falls in the sensing range of s_i, the $\zeta_{\alpha,i}^{\text{spa}}$ is 1; otherwise, the $\zeta_{\alpha,i}^{\text{spa}}$ is 0, i.e.,

$$\zeta_{\alpha,i}^{\text{spa}} = \begin{cases} 1, & d(\alpha, s_i) \le r_s \\ 0, & \text{otherwise.} \end{cases} \tag{19}$$

Let $d(\alpha, s_i)$ denote the Euclidean distance between point α and the sensor s_i. Let $\zeta_{i,t}^{\text{tem}}$ be a Boolean variable, indicating whether or not the sensor s_i performs a monitoring task at time t. If s_i is sensing at time t, then $\zeta_{i,t}^{\text{tem}}$ is 1; otherwise, $\zeta_{i,t}^{\text{tem}}$ is 0.

Let $\vartheta_{\alpha,t}$ denote spatial and temporal surveillance quality of the point α at time t. If the α is within the sensing range of sensor $s_i(\zeta_{\alpha,i}^{\text{spa}} = 1)$, and s_i is sensing at time $t(\zeta_{i,t}^{\text{tem}} = 1)$, $\vartheta_{\alpha,t}$ is 1; If the point α does not fall in the sensing range of sensor s_i, but s_i is monitoring at t, $\vartheta_{\alpha,t}$ is

$$\vartheta_{\alpha,t} = \begin{cases} (1-\kappa^{\text{spa}})^{d(\alpha,s_i)}, & \zeta_{\alpha,i}^{\text{spa}} = 0, \quad \zeta_{i,t}^{\text{tem}} = 1 \\ 0, & \text{otherwise.} \end{cases} \tag{20}$$

Let κ^{spa} denote the loss rate of spatial surveillance quality per unit of distance. Assume that point α falls in the sensing range of sensor s_i. Assume that s_i does not sensing at time t. Instead, it performs sensing operation at the time t_1 which is the nearest time point to time t. The value of $\vartheta_{\alpha,t}$ can be obtained by

$$\vartheta_{\alpha,t} = \begin{cases} (1-\kappa^{\text{tem}})^{d(t,t_1)}, & \zeta_{\alpha,i}^{\text{spa}} = 1, \zeta_{i,t_1}^{\text{tem}} = 1 \\ 0, & \text{otherwise.} \end{cases} \tag{21}$$

Let κ^{tem} denote the loss rate of temporal surveillance quality per unit of time. Let $d(t, t_1)$ denote the time difference between t and t_1. Assume that point α is outside the sensing range of the s_i. The value of $\vartheta_{\alpha,t}$ is

$$\vartheta_{\alpha,t} = \begin{cases} (1-\kappa^{\text{tem}})^{d(t,t_1)} \times (1-\kappa^{\text{spa}})^{d(\alpha,s_i)}, & \\ \qquad \zeta_{\alpha,i}^{\text{spa}} = 0, \quad \zeta_{i,t_1}^{\text{tem}} = 1 & \\ 0, \qquad \text{otherwise.} & \end{cases} \tag{22}$$

Let $\mathbb{Q}$ denote the data surveillance quality of all monitoring regions. We have

$$\mathbb{Q} = \sum_{\alpha \in R} \sum_{t \in T} \vartheta_{\alpha,t}. \tag{23}$$

The goal of this study is to find a recharging algorithm to maximize the data surveillance quality. Let $\mathcal{M}^{\text{best}}$ denote the best recharging algorithm and $\mathcal{M}$ denote a set of recharging algorithms. Equation (24) expresses the objective function of this study

Objective function

$$\mathcal{M}^{\text{best}} = \arg\max_{\mathcal{M}^{\text{best}} \in \mathcal{M}} \sum_{\alpha \in R} \sum_{t \in T} \vartheta_{\alpha,t}. \tag{24}$$

There are some constraints that need to be satisfied. The first constraint is the *energy of the MC*. The MC recharges the sensors by moving to the appointed location. Let $\mathcal{B}_M^{\text{move}}$ and $\mathcal{B}_M^{\text{rech}}$ denote the energy consumptions of the MC for moving along the recharging path and recharging the sensors, respectively. Equation (25) gives the energy constraint of the MC which ensures the MC gets to the base station and is recharged before its energy is exhausted.

1) MC Energy Constraint:

$$\mathcal{B}_M^{\text{move}} + \mathcal{B}_M^{\text{rech}} \le \mathcal{B}_M. \tag{25}$$

Another constraint is the *working efficiency constraint*. Each sensor moves to the RS for recharging. Recall that $\mathcal{B}_s^{\text{ford}}$ and $\mathcal{B}_s^{\text{back}}$ denote the energy required for the sensor's travel to and from the RS, respectively. Let $\mathcal{B}_s^{\text{rem}}$ denote the remaining battery energy for monitoring work. Equation (26) ensures that the most energy is used for the monitoring task.

2) Working Efficiency Constraint:

$$\mathcal{B}_s^{\text{rem}} \gg \mathcal{B}_s^{\text{ford}} + \mathcal{B}_s^{\text{back}}. \tag{26}$$

Another constraint is the *data freshness constraint*. Starting from the base station, the MC arrives at the RS for recharging the sensors and simultaneously collects the sensing data from the sensors. Along the recharging path, the MC finally gets back to the base station for recharging itself and transmits sensing data to the base station. Let Γ_M^{move} and Γ_M^{rech} denote the moving time and the recharging time of the MC along the recharging path for a round, respectively. Let Γ denote the data freshness threshold. Equation (27) ensures that the data received by the base station satisfies the data freshness constraint.

3) Data Freshness Constraint:

$$\Gamma \le \Gamma_M^{\text{move}} + \Gamma_M^{\text{rech}}. \tag{27}$$

The goal of this article is to develop a recharging algorithm that aims to achieve the objective function given in (24) and satisfies the constraints given in (25)–(27).

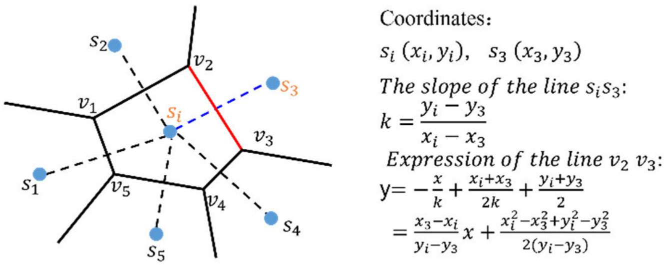

Fig. 2. Voronoi cell of sensor s_i.

IV. Algorithm Description

This study proposes a recharging algorithm that aims to maximize the surveillance quality of the monitoring region. The algorithm mainly consists of three phases: the sensors relocation (SR) phase, the RS number and location determination (RSNL) phase, and the batching recharging (BR) phase. In the SR phase, sensors are evenly relocated, aiming to balance spatial surveillance quality. In the RSNL phase, the proposed algorithm divides the monitoring area into equal-sized subregions, aiming to determine the number and locations of RSs. In the BR phase, the proposed algorithm calculates the starting recharging time of each RS and broadcasts it to all the sensors in that subregion. In addition, the sensors are recharged by the MC according to the working time and recharging interval.

A. SR Phase

The sensor nodes are randomly deployed in the monitoring region. Some areas have many nodes, while other areas may have few nodes. To balance the distances between sensors, this study adopts the expelling and attractive force approach to achieve a more balanced distribution of sensors. When two nodes are too close, there should be a repulsive force to push them away from each other. On the contrary, if two nodes are too far apart, there should be an attractive force to bring them closer together. However, one sensor might be a neighbor to many sensors. The overall force on the node is the vector sum of all the expelling and attractive forces from neighboring nodes.

The study assumes that the sensors are aware of themselves and neighbors' location information. It is easy to realize by installing the GPS on the sensors [22]. Let V_i denote the Voronoi cell of sensor s_i. As shown in Fig. 2, based on the neighboring sensors s_1, s_2, s_3, s_4, and s_5, sensor s_i can construct its Voronoi cell V_i. The perpendicular bisectors between the s_i and its Voronoi neighbors form the solid edges of the V_i. In V_i, each point is closer to the sensor s_i, as compared with the other sensors.

Let $d(s_i, s_j)$ denote the distance between sensor s_i and s_j. Let d_{ave} denote the average distance between all pairs of two sensors in the monitoring region. The notation d_{ave} can be calculated in advance because the size of the monitoring region and the number of sensors are known [22].

In case that condition $d(s_i, s_j) < d_{\text{ave}}$ holds, nodes s_i and s_j should be away from each other with distance $(d_{\text{ave}} - d(s_i, s_j))/2$. On the other hand, if condition $d(s_i, s_j) > d_{\text{ave}}$, nodes s_i and s_j should be closer with a distance of $(d(s_i, s_j) - d_{\text{ave}})/2$. Since each sensor can calculate its distance and direction to neighboring sensors, the distance between sensors will be balanced in a distributed manner. Let $\vec{F}_{ji}$ denote the virtual force from sensor s_j to sensor s_i. The value of $\vec{F}_{ji}$ can be calculated as shown in the following equation:

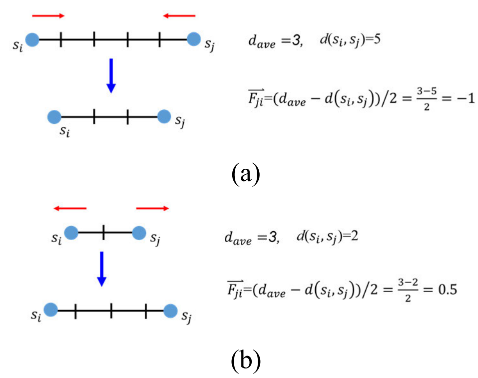

Fig. 3. Attracting and expelling forces between two nodes. (a) Attracting force. (b) Expelling force.

$$\left|\vec{F}_{ji}\right| = \left|d_{\text{ave}} - d\left(s_i, s_j\right)\right| \Big/ 2. \tag{28}$$

Assume that N_i denotes the set of neighboring sensors of s_i. The total force, denoted by $\vec{F}_i$ can be presented as shown in the following equation:

$$\vec{F}_i = \sum_{s_j \in N_i} \vec{F}_{ji}. \tag{29}$$

Fig. 3 provides examples of attractive and expelling forces between two nodes. In Fig. 3(a), assuming $d_{\text{ave}} = 3$, and $d(s_i, s_j) = 5$, it is very evident that the distance between the s_i and s_j is greater than the average distance. Therefore, the two nodes experience an attractive force with a strength of -1, indicating that the nodes move 1 unit toward each other. In Fig. 3(b), $d(s_i, s_j) = 2$, which is less than the average distance. As a result, s_i and s_j experience an expelling force with a strength of 0.5, causing each node to move 0.5 units away from each other.

Fig. 4 gives an example to show the computation of the total force of sensor s_i. As shown in Fig. 4, the sensor s_i has three neighbor nodes s_1, s_2, and s_3. Since we have

$$\begin{aligned} &d(s_i, s_1) > d_{\text{ave}} \\ &d(s_i, s_3) > d_{\text{ave}}, \quad \text{and} \\ &d(s_i, s_2) < d_{\text{ave}}. \end{aligned}$$

To balance the distances of s_i and s_1, s_2, and s_3. The sensor s_i should move closer to s_1 and s_3 but should move far away from s_2. Therefore, s_1 and s_3 exert the attractive force, and s_2 exerts the expelling force on the s_i, which are shown by the orange, purple, and blue lines in Fig. 4(a), respectively. In Fig. 4(b), the red line represents the overall force on s_i.

Let s_j be the neighbors of s_i. Let notations $\mathcal{G}_{s_i}$ and $\mathcal{G}^{\text{nei}}_{s_i,s_j}$ denote the areas of the V_i and V_j, respectively. Let σ denote the threshold. The virtual forces computation and sensors

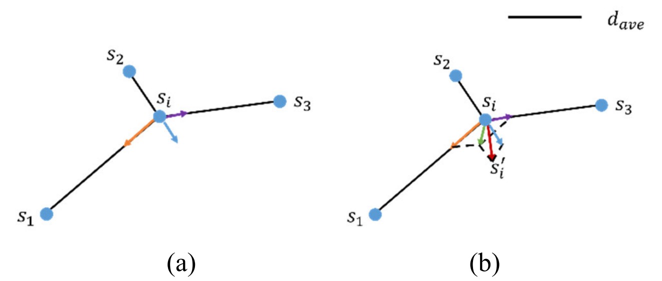

Fig. 4. Force on the sensor s_i. (a) Three forces on the s_i. (b) Overall force on the s_i.

movement can be repeatedly executed until condition (30) is satisfied

$$\min_{s_j \in N_i} \left(\mathcal{g}_{s_i} - \mathcal{g}^{\text{nei}}_{s_i,s_j} \right) \le \sigma. \tag{30}$$

B. RS Number and Location Determination Phase

In the proposed algorithm, all sensors will move to the closest RS. In the conceptual design, the sensors, MCs, and RSs act like people, buses, and bus stations, respectively. The people who want to take the bus must go to the closest bus station. There might be several buses moving along the same path, which passes through all bus stations. Similarly, all sensors aiming to be recharged should move to the RS for recharging. There is a path passing through all RSs and recharging those sensors which have already arrived at the RS. This phase aims to determine the number and the locations of the RSs.

To achieve this, the proposed algorithm initially partitions the whole monitoring region into m subregion. One MC will be dispatched to each subregion for recharging the sensors deployed in that specific area. To minimize the movement costs of sensors from their sensing locations to the RSs, there may be multiple RSs in each subregion. For simplicity, each subregion will be further divided into k clusters, with each cluster having one RS deployed.

Assumes that the MC consumes $1/m$ of its total energy for recharging and moving in each subregion. The number of RSs can impact the surveillance quality and recharging efficiency of the MC. Having a large number of RSs can significantly reduce the average movement distance between sensors and RSs. However, this policy will consume too much energy of the MC since it should move to each RS. In addition, this policy also has the disadvantage of low recharging efficiency. Extensively deploying the RSs will decrease the number of sensors recharging simultaneously at each station. As a result, the number of sensors that can be simultaneously recharged is also decreased, leading to low recharging efficiency. In addition, each RS also needs to occupy a fixed recharging time in the recharging cycle. In consequence, the time cycle for the MC to travel all RSs will be extended, resulting in dissatisfying the data freshness constraint or no time to recharge some sensors. Therefore, the number of RSs should be carefully planned.

Therefore, assume that each subregion has k virtual RSs. The density of the RSs is $\rho = (k/(L \times M/m))$ in the subregion. Therefore, the average distance between the two adjacent RSs is $d = \sqrt{2/\rho}$ [23]. Two major opportunities that the MC consumes its energy: moving and recharging. Let notations $\mathcal{B}^{\text{rech}}_{M,\text{reg}}$ and $\mathcal{B}^{\text{move}}_{M,\text{reg}}$ denote the energy cost for recharging and moving in the subregion, respectively. The energy consumption of the MC must satisfy the following equation:

$$\mathcal{B}^{\text{rech}}_{M,\text{reg}} + \mathcal{B}^{\text{move}}_{M,\text{reg}} \le \frac{1}{m} \times \mathcal{B}_M. \tag{31}$$

This study assumes that when the sensors reach to the RS for recharging, they just exhaust their energy. In this way, the most energy can be reserved for sensors to execute the monitoring task, aiming to maximize the surveillance quality. Recall that $\mathcal{B}_s$ denotes the total energy of sensor s. Let ℓ denote the recharging efficiency rate of the MC. The MC needs to consume $(k\mathcal{B}_s/\ell)$ energy for each subregion, i.e.,

$$\mathcal{B}^{\text{rech}}_{M,\text{reg}} = \frac{k\mathcal{B}_s}{\ell}. \tag{32}$$

Furthermore

$$\mathcal{B}^{\text{move}}_{M,\text{reg}} = (k+1) \times d \times e^{\text{move}}_M. \tag{33}$$

Based on (31)–(33), the upper bound of the notation k is calculated

$$k \le \frac{\ell \times \left(\mathcal{B}_M - d \times m \times e^{\text{move}}_M\right)}{m\left(\mathcal{B}_s + d \times \ell \times e^{\text{move}}_M\right)}. \tag{34}$$

Next, the lower bound of k is concerned. A smaller number of RSs leads to shorter recharging paths for the MC and enables more sensors to be recharged simultaneously at each RS, enhancing the recharging efficiency. However, this policy also results in the longer average distance between the mobile sensors and the RSs. Consequently, the mobile sensors need to move long distances to reach the RS for recharging, causing them to allocate more energy for movement. Therefore, it is essential to avoid having too few RSs. The following outlines the calculation method for determining the lower bound of the notation k.

The working efficiency constraint, as stated in (35), can be rewritten as

$$\mathcal{B}^{\text{rem}}_s > \varepsilon\left(\mathcal{B}^{\text{ford}}_s + \mathcal{B}^{\text{back}}_s\right) \tag{35}$$

where ε is a constant greater than 10. Equation (36) calculates the $\mathcal{B}^{\text{rem}}_s$

$$\mathcal{B}^{\text{rem}}_s = \mathcal{B}_s - \left(\mathcal{B}^{\text{ford}}_s + \mathcal{B}^{\text{back}}_s\right). \tag{36}$$

Without the loss of generality, the longest distance that the sensor can move is the diagonal distance in the grid. Therefore,

$$\begin{aligned} \mathcal{B}^{\text{ford}}_s + \mathcal{B}^{\text{back}}_s &\le 2 \times e^{\text{move}}_s \times \sqrt{\frac{M^2}{(mk)^2} + \frac{L^2}{(mk)^2}} \\ &= \frac{2 \times e^{\text{move}}_s \times \sqrt{M^2 + L^2}}{mk}. \end{aligned} \tag{37}$$

According to (35)–(37), the lower bound of the notation k is calculated

$$k \ge \frac{2(\varepsilon+1) \times e^{\text{move}}_s \times \sqrt{M^2+L^2}}{m\mathcal{B}_s}. \tag{38}$$

Notation k is the integer between the upper bound and lower bound

$$\left\lceil \frac{2(\varepsilon+1)\times e_s^{\text{move}}\times\sqrt{M^2+L^2}}{m\mathcal{B}_s}\right\rceil \leq k \leq \left\lfloor \frac{\ell\times\left(\mathcal{B}_M-d\times m\times e_M^{\text{move}}\right)}{m\left(\mathcal{B}_s+d\times l\times e_M^{\text{move}}\right)}\right\rfloor. \quad (39)$$

Therefore, the feasible solutions for variable k are obtained. This indicates that the number of RSs can be determined. The next issue is to determine the location of each RS.

The key concept for determining the locations of k RSs is to apply the K-means algorithm to the sensors in each subregion. This indicates that the sensors in each subregion should be partitioned into k clusters and the RS will be deployed at the center location of each cluster. Initially, in each subregion, k clustering points are randomly selected. Then, the clustering operation is performed based on the distances between the clustering points and sensors. Then, for each cluster, its centroid is determined, and the nearest point to the centroid will play the role of clustering point. These steps will be repeatedly applied until the members of each cluster remain unchanged. Finally, the centroid of each cluster is set as an RS, and the centroid near the center of the monitoring area is set as the base station.

C. BR Phase

According to the location of the RS_j, the shortest recharging path of the MC is constructed based on the TSP algorithm for the monitoring region. Then the shortest recharging path is evenly divided into m segments. Let $\text{RS}_i^{\ell}(1 \leq i \leq m, 1 \leq \ell \leq k)$ denote the RSs of the ith MC which aims to move in the ith subregion. For instance, RS_2^1 denote the first RS of the second MC which aims to move in the second subregion. Next, this study calculates the starting recharging time of the first RS in the ith subregion. Based on this, this study then calculates the starting recharging time for each RS.

Assumed that there are u sensors, denoted by $S_i^1 = \{s_{i,1}^1, s_{i,2}^1, \ldots, s_{i,u}^1\}$, in the cluster of RS_i^1. Let $l_{s_{i,j}^1}$ denote the location of the sensor $s_{i,j}^1$. Let $d(x, y)$ denote the Euclidean distance between x and y. Let $\mathcal{B}_{\text{RS}_i^1,s_{i,j}^1}^{\text{move}}$ denote the energy consumption of the sensor $s_{i,j}^1$ for moving from $s_{i,j}^1$ to RS_i^1. The value of $\mathcal{B}_{\text{RS}_i^1,s_{i,j}^1}^{\text{move}}$ can be obtained by the following equation:

$$\mathcal{B}_{\text{RS}_i^1,s_{i,j}^1}^{\text{move}} = d\left(l_{s_{i,j}^1}, \text{RS}_i^1\right)\times e_s^{\text{mov}}. \quad (40)$$

Let $\mathcal{B}_{\text{RS}_i^1,s_{i,j}^1}^{\text{rem}}$ denote the remaining energy of the sensor $s_{i,j}^1$ for executing monitoring work. Notation $\mathcal{B}_{\text{RS}_i^1,s_{i,j}^1}^{\text{rem}}$ can be calculated by the following equation:

$$\mathcal{B}_{\text{RS}_i^1,s_{i,j}^1}^{\text{rem}} = \mathcal{B}_s - \mathcal{B}_{\text{RS}_i^1,s_{i,j}^1}^{\text{move}}. \quad (41)$$

Let $T_{\text{RS}_i^1,s_{i,j}^1}^{\text{rech}}$ denote the time period required for the sensor $s_{i,j}^1$ being recharged by the MC. The $T_{\text{RS}_i^1,s_{i,j}^1}^{\text{rech}}$ can be obtained by applying the following equation:

$$T_{\text{RS}_i^1,s_{i,j}^1}^{\text{rech}} = \frac{\mathcal{B}_{\text{RS}_i^1,s_{i,j}^1}^{\text{rem}}}{e_j^{\text{work}}}. \quad (42)$$

To satisfy the recharging requirement of each sensor and improve the surveillance quality, this study assumes that the starting recharging time of the RS_i^1 is the time minimize the recharging time of the $s_{i,j}^1$. That is,

$$T_{\text{RS}_i^1}^{\text{start\_ch}} = \min_{s_{i,j}^1\in s_i^1}\left(T_{\text{RS}_i^1,s_{i,j}^1}^{\text{rech}}\right), \quad (1\leq i\leq m, 1\leq j\leq u). \quad (43)$$

Based on the value of $T_{\text{RS}_i^1}^{\text{start\_ch}}$, the starting recharging time of the other RS is calculated by (44). Let $T_{\text{RS}_i^{\ell}}^{\text{start\_ch}}$ denote the starting recharging time of RS_i^{ℓ}. The value of the $T_{\text{RS}_i^{\ell}}^{\text{start\_ch}}$ is can be calculated by applying the following equation:

$$T_{\text{RS}_i^{\ell}}^{\text{start\_ch}} = T_{\text{RS}_i^{\ell-1}}^{\text{start\_ch}} + \frac{\mathcal{B}_s}{\ell\times e_M^{\text{ch}}} + \frac{d\left(\text{RS}_i^{\ell-1}, \text{RS}_i^{\ell}\right)}{v_M}. \quad (44)$$

As previously mentioned, the study applied the K-means algorithm to divide the whole monitoring region into the $m \times k$ clusters, denoted by $C = \{c_1, c_2, \ldots, c_{m\times k}\}$. At the starting recharging time, all sensors move to the RS_i for being recharged in the c_i. This implies that the recharging sensors cannot work and results in low surveillance quality of the c_i. To improve the surveillance quality, this study assumes that the recharging tasks of sensors are arranged in batches. Let Θ_i denote the number of the batches of the sensors in the c_i. As shown in (45), the value of the notation Θ_i is equal to average working time of the sensors in the c_i devided by recharging interval of the c_i which is an integer

$$\Theta_i = \left\lceil \frac{\text{average}\left(T_{\text{RS}_i^{\ell},s_{i,j}^{\ell}}^{\text{work}}\right)}{T_{\text{RS}_i^{\ell}}^{\text{start\_ch}} - T_{\text{RS}_i^{\ell}}^{\text{start\_ch}'}}\right\rceil \quad (45)$$

where $T_{\text{RS}_i^{\ell}}^{\text{start\_ch}'}$ denotes the next starting recharging time of the RS_i^{ℓ}.

After sensors are recharged in batches, the recharging time is Θ_i times later compared to recharging without batching. To ensure that the sensors do not deplete their battery before being recharged by the MCs, this article adjusts the sensing frequency of sensors based on the starting recharging time of sensor. Let $\mathcal{B}_i^{\text{ses}}$ denote the energy consumption of sensor s_i when performing one sensing task. The value of $\mathcal{B}_i^{\text{ses}}$ can be calculated by the following equation:

$$\mathcal{B}_i^{\text{ses}} = \frac{e_i^{\text{work}}}{f_i}. \quad (46)$$

Let $\mathcal{B}_i^{\text{work}}$ denote the energy reserved for s_i to execute the sensing task. Sensor s_i needs to travel to the corresponding RS to be recharged by the MC. After that the MC completes the recharging process, the sensor then returns to its original work location to resume the monitoring operations. The value of $\mathcal{B}_i^{\text{work}}$ can be determined using the following equation:

$$\mathcal{B}_i^{\text{work}} = \mathcal{B}_s - 2\times d(l_{s_i}, \text{RS}_i)\times e_s^{\text{move}}. \quad (47)$$

Let $\mathbb{N}_i^{\text{ses}}$ denote the number of sensor detections, where $\mathbb{N}_i^{\text{sensing}}$ is equal to $\mathcal{B}_i^{\text{rem}}$ divided by $\mathcal{B}_i^{\text{sensing}}$

$$\mathbb{N}_i^{\text{ses}} = \frac{\mathcal{B}_i^{\text{rem}}}{\mathcal{B}_i^{\text{ses}}}. \quad (48)$$

Inputs: The unique ID, $\mathcal{B}_M$, $\mathcal{B}_s$, $l_{s^1_{i,j}}$, e_s^{move}, e_i^{work}, v_M.	
Output: k, RSs locations, $T^{start\_ch}_{RS_i^{\mathfrak{f}}}$, Θ_i, f_i^{new}.	
1	/* RS Phase */
2	Evenly distribute randomly deployed sensors according to Exps. (28) - (29);
3	if(Exp. (30)){
4	The distribution of sensors is approximately balanced;}
5	else{
6	The virtual forces computation and sensors movement can be repeatedly executed;}
7	/* RSNL phase */
8	Calculate the number of RS in each sub-region based on Exp. (39);
9	Determine the locations of RSs applying the K-means algorithm;
10	/* BR Phase*/
11	According to the location of the RS_j, the shortest recharging path of the mobile charger is constructed based on the TSP algorithm;
12	The shortest recharging path is evenly divided into m segments;
13	Calculate the starting recharging time of every RS according to Exp. (40) – (44);
14	To improve the surveillance quality, sensors are recharged in batches according to Exp. (45);
15	/* After batch recharging of the sensors, the recharging time is delayed compared to non-batched recharging. To ensure that the sensors do not deplete their energy before being recharged, the sensing frequency of the sensors has been adjusted. */
16	Apply Exp. (46) – (50) for adjusting the sensing frequency of sensors.

Fig. 5. Pseudocode of the proposed algorithm.

Let T_i^{work} denote the working time of s_i. The value of T_i^{work} is calculated by the following equation:

$$T_i^{\text{work}} = T^{\text{start\_ch}}_{\text{RS}_i^{\mathfrak{f}}} - 2 \times \frac{d(l_{s_i}, \text{RS}_i)}{v_s}. \tag{49}$$

Let f_i^{new} denote the adjusted working frequency of the s_i. The value of f_i^{new} is calculated by the following equation:

$$f_i^{\text{new}} = \frac{\mathbb{N}_i^{\text{ses}}}{T_i^{\text{work}}}. \tag{50}$$

The following outlines the proposed algorithm as illustrated in Fig. 5.

The time complexity of the proposed algorithm mainly comes from the computations in the SR, RSNL, and BR phases. In the SR phase, the computation involves iterative calculations of attraction–repulsion forces and the construction of a Voronoi diagram. The per-iteration complexity of attraction–repulsion forces is $O(n \cdot \hbar)$, where n is the number of sensors and $\hbar$ represents the average number of neighbor nodes, typically $\hbar \ll n$. The time complexity for constructing the Voronoi diagram is $O(n \log n)$. Let T_{SR} denote the total time cost of the SR phase, and w represent the number of iterations. The value of T_{SR} is calculated using the following equation:

$$T_{\text{SR}} = O(w \cdot n \log n). \tag{51}$$

During the RSNL phase, the main computational tasks include determining the constraints for the number of RSs and performing K-means clustering for RS placement. Recall that notation m is the number of subregions and notation k is the number of clusters in each subregion. The time complexity of the RS quantity constraint is $O(mk)$. In this study, the monitoring space is considered as a 2-D space. The time complexity of K-means clustering is $O(2n \cdot mk \cdot \mathfrak{h})$, where $\mathfrak{h}$ is the number of iterations. Let T_{RSNL} denote the total time cost in the RSNL phase, which is calculated by the following equation:

$$T_{\text{RSNL}} = O(mk) + O(2n \cdot mk \cdot \mathfrak{h}). \tag{52}$$

During the BR phase, the main tasks include TSP-based path planning, batch charging of sensors, and monitoring frequency adjustment, with time complexities of $O(mk^2 \cdot 2^{mk})$, $O(n)$, and $O(n)$, respectively. Let T_{BR} denote the total time cost in the BR phase. The value of T_{BR} can be obtained by the following equation:

$$\begin{aligned} T_{\text{BR}} &= O\left((mk)^2 \cdot 2^{mk}\right) + O(n) + O(n) \\ &= O\left((mk)^2 \cdot 2^{mk} + n\right). \end{aligned} \tag{53}$$

Let T_{total} represent the total time complexity of the proposed algorithm, which equals the sum of the complexities from the SR, RSNL, and BR phases. The value of T_{total} is calculated by the following equation:

$$\begin{aligned} T_{\text{total}} &= O(wn \log n) + O(mk) + O(2n \cdot mk \cdot \mathfrak{h}) \\ &\quad + O\left((mk)^2 \cdot 2^{mk} + n\right) \\ &= O\left(wn \log n + 2n \cdot mk \cdot \mathfrak{h} + (mk)^2 \cdot 2^{mk}\right). \end{aligned} \tag{54}$$

V. Performance Evaluation

In this study, all sensors and MCs are mobile. Their collaboration can reduce the distance traveled by the MCs. This study uses the ISAC-Assisted WRSNs with multiple MCVs algorithm (ISACM) [19], redundant mobile sensors dispatch and cascaded movement algorithm (RMSDCM) [20], and the flexible charging protocol (FCP) [21] as the benchmarks for comparison in terms of performance. Both RMSDCM and FCP algorithms involve mobile sensors.

The ISACM algorithm employed multiple MCs to wirelessly charge sensors, aiming to enhance charging efficiency. The ISACM adopted a charging load strategy to evenly distribute tasks across MCs. This strategy evaluated four parameters: the sensor's residual energy, the MC-sensor distance, the neighbor node count, and the sensor's betweenness centrality. Meanwhile, the algorithm applied the charging factor strategy to enable efficient partial charging for the monitoring region. Additionally, it applied the ISAC technology to reduce the travel time of MC, lower charging costs, and further enhance energy use efficiency.

The RMSDCM algorithm aims to prolong the lifetime of WRSNs or maximize the shortest effective monitoring time. When sensors with low battery levels travel to RSs for energy replenishment, the algorithm allocates redundant sensors to replace them and perform monitoring tasks. The RMSDCM algorithm assigns weights based on the residual energy of sensors, which is calculated as the difference between the sensor's current energy and the energy required to reach the RS. Sensors with lower remaining energy are assigned higher weights, corresponding to higher priority levels. When the number of redundant sensors is insufficient, the algorithm allocates them based on the sensors' weights, prioritizing those with higher weights. If no redundant sensors are available for allocation, the algorithm balances energy levels by cascading the movement of sensors, whereby sensors with higher energy levels replace those with lower energy levels to carry out the monitoring tasks.

The FCP algorithm divides the monitoring area into a movement region and an energy transfer region, where the movement region includes the recharging zones. The algorithm employs sensors to recharge other sensors, aiming to extend the lifecycle of the WRSNs. The FCP algorithm stipulates that the sensors within the recharging area can convert natural energy into electrical energy for self-recharging. Once recharged, they move to the boundary of the mobile area to transfer energy to sensors located in the boundary energy transfer area. Other sensors within the transfer area obtain energy from their upstream neighboring nodes.

However, both RMSDCM and FCP algorithms assume complete coverage of the monitoring region, which is a rather stringent assumption. To ensure fairness, modifications were made to these algorithms. Taking into account that each sensor has its own monitoring task, the modified-RMSDCM algorithm specifies that when a sensor is recharging, neither redundant sensors NOR cascaded sensors are available to assist with monitoring. The sensor resumes its monitoring duties at its original location once fully recharged. The modified-FCP algorithm stipulates that when sensors in the recharging area act as MCs to recharge sensors in other areas, they will be unable to perform the monitoring task. In the experimental stage, surveillance quality and recharging efficiency are compared. Below, the experimental environment is described first, followed by a discussion of the results.

A. Simulation Environment

As shown in Fig. 6, the area of the monitoring region is set to 1000 × 1000 m, and the sensors are randomly deployed in the monitoring area. The recharging rate of the MC is 2 J/s. The energy consumption of the MC ranges from 0.3 to 0.9 J/m when moving. The monitoring radius of the sensor is between 10 and 30 m, the battery capacity ranges from 100 to 500 KJ, and the moving speed is 0.3 m/s. Other specific parameters are shown in Table II.

B. Simulation Results

In this study, sensors move to the RSs at the rendezvous time to be recharged by the MCs. As described in Section IV, to enhance the surveillance quality, this study arranges the sensors to be recharged in batches. A recharging cycle is defined as the comprehensive completion of the recharging

TABLE II
SIMULATION SETTINGS

Parameters	Values
Monitoring region	1000 m×1000 m
Deployment	Randomly
e_M^{ch}	2J/s
e_M^{move}	0.3-0.9J/m
v_M	1m/s
r_s	10-30m
$\mathcal{B}_s$	100-500KJ
v_s	0.3m/s
e_s^{move}	0.1-0.3J/m
κ^{tem}	0.1
κ^{spa}	0.3

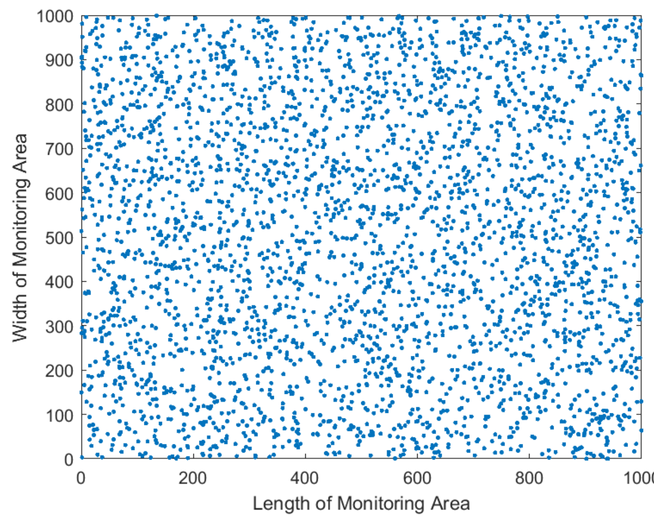

Fig. 6. Scenario where sensors are randomly deployed in the monitoring area.

process for all sensors. Let T_{round} denote the time of one round. Let $\mathcal{N}$ denote the number of rounds within a certain monitoring time T. The value of $\mathcal{N}$ is calculated by the following equation:

$$\mathcal{N} = \frac{T}{T_{\text{round}}}. \tag{55}$$

Let $\mathcal{B}_s^{\text{move}}$ denote the energy consumption of all the sensors that need to move for recharging within time T. The value of $\mathcal{B}_s^{\text{move}}$ is equal to the round-trip moving energy consumption of all sensors to the RSs multiplied by $\mathcal{N}$. The energy associated with sensors movement includes the energy expended to move to the RSs for recharging and the energy consumed to return to the monitoring positions after recharging

$$\mathcal{B}_s^{\text{move}} = \mathcal{N} \times \sum_{i=1}^{n} \sum_{j=1, i\neq j}^{mk} \left(2 \times d\left(l_{s_i}, \text{RS}_j\right) \times e_s^{\text{move}}\right). \tag{56}$$

Fig. 7 compares $\mathcal{B}_s^{\text{move}}$ when the monitoring area is divided into a different number of partitions. In Fig. 7, the monitoring area is divided into two subregions, each of which is further divided into k equal partitions, with k taking the values 5, 10, and 15. To improve recharging efficiency, the proposed algorithm arranges for all sensors to move to the nearest RS for recharging. To determine the number and locations of RSs,

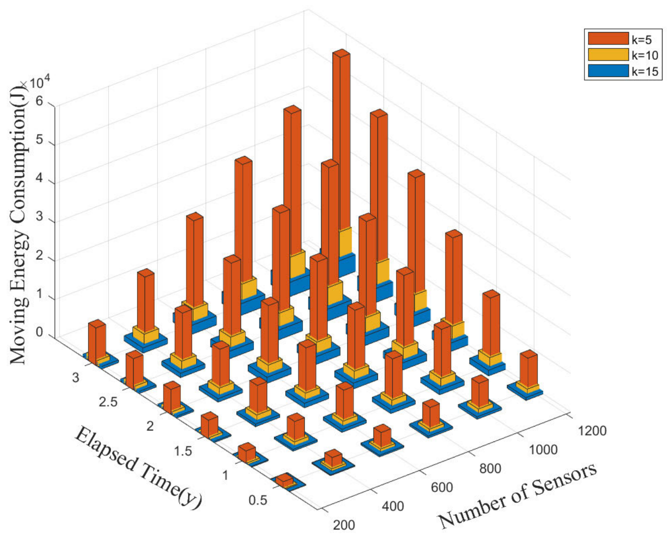

Fig. 7. Comparing energy consumption of sensors when moving for recharging by considering different elapsed times and number of sensors.

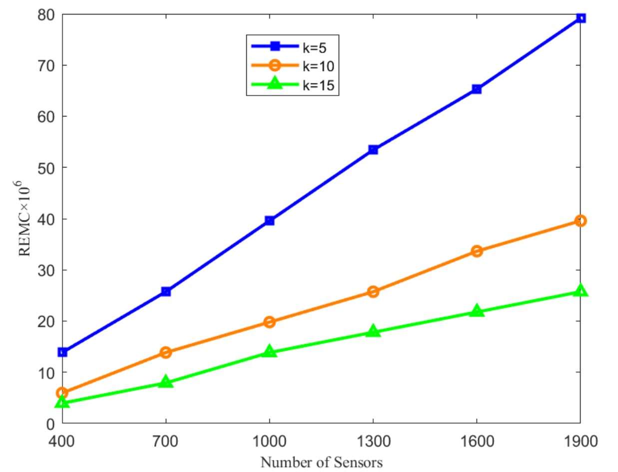

Fig. 8. Comparing the recharging efficiency of MCs for different numbers of sensors.

this algorithm divides the monitoring area into subregions. Each subregion is assigned the MC to provide recharging services. Furthermore, to minimize the moving distance of sensors from the sensing location to the RS, each subregion is further subdivided into equally sized partitions. The range of elapsed time spans from 0.5 to 3 years. As illustrated in Fig. 5, a smaller value of k indicates a smaller number of RSs. This leads to the increased energy consumption of sensors for movement to RSs. In contrast, a larger value of k decreases energy consumption. This phenomenon can be attributed to the proximity of sensors to the RSs when k is larger, thereby reducing the energy required for movement and conserving more energy for monitoring tasks. Conversely, when k is smaller, sensors are farther from the RSs, which leads to higher energy consumption for movement and less energy available for monitoring. The proposed algorithm sets a lower limit for k to prevent it from being excessively small, thereby ensuring that a greater proportion of the sensor's battery is allocated to monitoring rather than movement.

Let REMC denote the recharging efficiency of the MC over one recharging cycle. Let ψ denote the number of partitions that the MCs need to visit in one recharging cycle. The value of ψ can be obtained by (57). Let $\mathcal{B}_{M,r}^{\text{move}}$ and $\mathcal{B}_{M,r}^{\text{rech}}$ denote the energy consumed for moving and recharging of the MCs within one recharging round, respectively. The values of $\mathcal{B}_{M,r}^{\text{move}}$ and $\mathcal{B}_{M,r}^{\text{rech}}$ are calculated using (58) and (59), respectively. The value of REMC is determined by (60), where $\mathfrak{H}_{\hbar}$ denote the number of sensors recharged simultaneously in the $\hbar$th partition

$$\psi = \sum_{i=1}^{mk} \Theta_i \tag{57}$$

$$\mathcal{B}_{M,r}^{\text{move}} = \sum_{i=1}^{\psi} \sum_{j=2, i \neq j}^{\psi} e_M^{\text{move}} \times d(\text{RS}_i, \text{RS}_j) \tag{58}$$

$$\mathcal{B}_{M,r}^{\text{rech}} = \frac{\mathcal{B}_s}{\ell} \times \psi \tag{59}$$

$$\text{REMC} = \frac{\sum_{\hbar=1}^{\varphi} \mathfrak{H}_{\hbar}}{\mathcal{B}_{M,r}^{\text{move}} + \mathcal{B}_{M,r}^{\text{rech}}}. \tag{60}$$

Fig. 8 examines the REMC as the number of sensors increases from 400 to 1900. It is evident that when the parameter k increases, REMC decreases. Conversely, when k decreases, REMC increases. This trend arises because a larger k divides the monitoring area into more partitions, resulting in more RSs. Therefore, the MCs need to visit more RSs, increasing power consumption. Simultaneously, when the number of partitions increases, the number of sensors recharged simultaneously in each partition decreases, leading to a decrease in REMC. Conversely, with a smaller k, there are fewer RSs to visit, reducing energy consumption. Additionally, a smaller k increases the number of sensors being recharged simultaneously in each partition, thereby improving the REMC.

Recall that $\mathcal{G}_{s_i}$ and $\mathcal{G}_{s_i,s_j}^{\text{nei}}$ represent the areas of the Voronoi cells for sensor s_i and its neighbor s_j, respectively. Recall that notation σ represents the minimum difference area between $\mathcal{G}_{s_i}$ and $\mathcal{G}_{s_i,s_j}^{\text{nei}}$. Fig. 9 aims to compare the spatial surveillance quality of the monitoring region when σ is set at 5%, 10%, and 15%. The number of sensors varies ranging from 400 to 1600, and the elapsed time spans from 0.5 years to 2.5 years. As shown in Fig. 8, the spatial surveillance quality is increased with the number of sensors. In comparisons, the monitoring quality at $\sigma = 5\%$ is higher than that at $\sigma = 10\%$ and $\sigma = 15\%$. This improvement is attributed to the fact that a smaller σ indicates a more uniform distribution of sensors, thereby enhancing the spatial surveillance quality of the monitoring region.

In Fig. 10(a), eight randomly selected locations in the monitoring area are used to study the monitoring quality. They are numbered from 1 to 8 in a clockwise order from left to right. The proposed algorithm in this study consists of three phases: SR phase, RSNL phase and BR phase, which are represented by P1, P2, and P3, respectively. Fig. 10(b) shows the ablation study of this algorithm and compares their performance in terms of surveillance quality. In the figure,

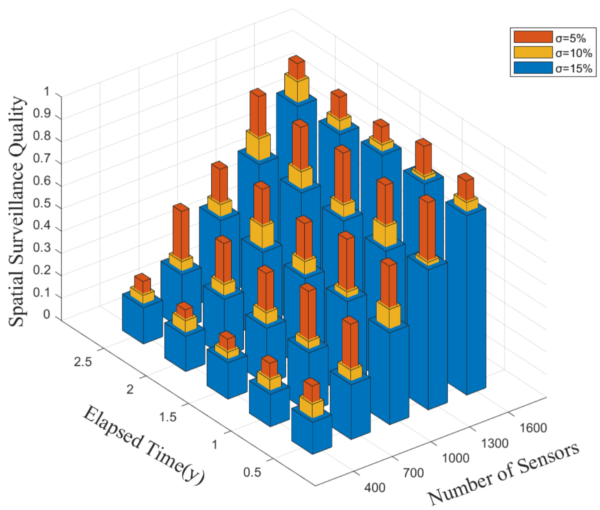

Fig. 9. Comparing the spatial surveillance quality of different σ by considering different numbers of sensors and varying elapsed time.

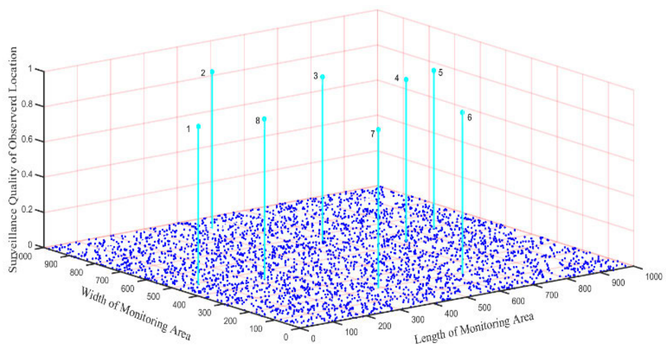

(a)

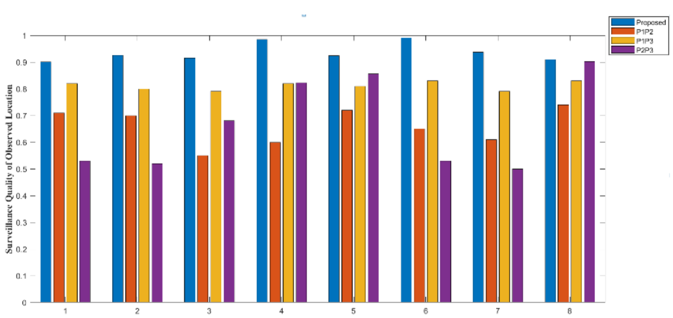

(b)

Fig. 10. Ablation study of the proposed algorithm. The proposed algorithm is compared with P1P2, P1P3, and P2P3 in terms of surveillance quality by considering eight selected locations. (a) Randomly selecting eight locations. (b) Surveillance quality comparison of the eight locations in the ablation experiment.

P1P2, P1P3, and P2P3 represent the approach after removing phases P3, P2, and P1, respectively.

As shown in Fig. 10(b), the surveillance quality of the proposed algorithm outperforms that of P1P2, P1P3, and P2P3. This phenomenon occurs because the P1P2 algorithm does not account for situations where all sensors in a cluster go for charging, rendering them unable to perform monitoring tasks during that period, thereby reducing monitoring quality. In the P1P3 algorithm, the number and locations of the RS are not optimized. An insufficient number of RS increases

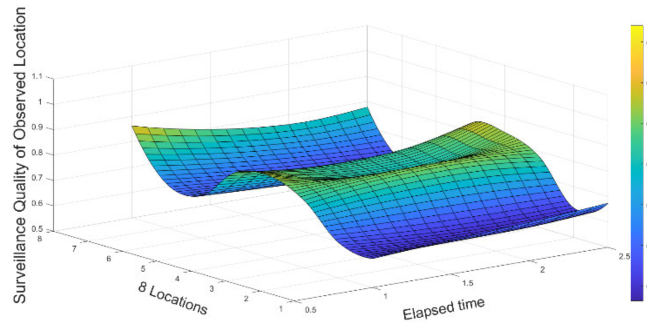

(a)

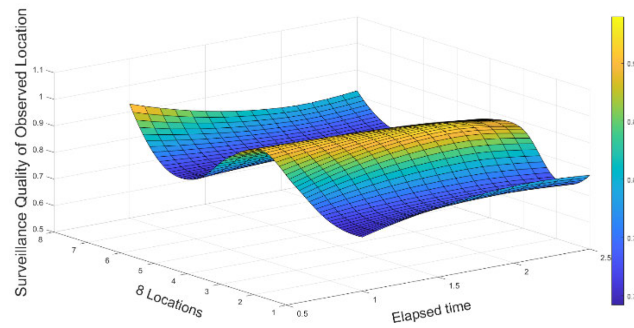

(b)

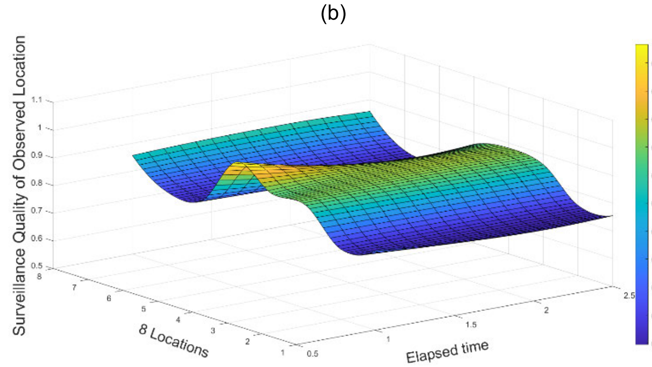

(c)

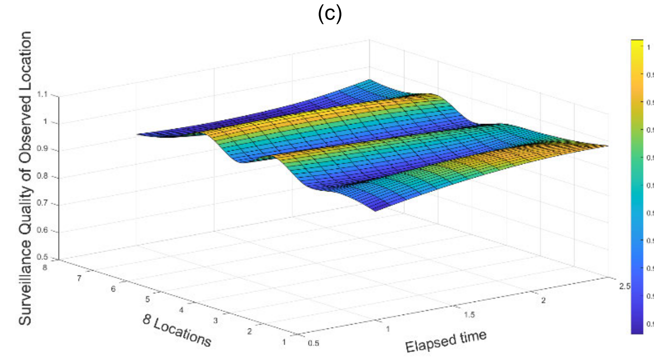

(d)

Fig. 11. Comparison of proposed algorithm, ISACM, modified-RMSDCM, and modified-FCP in terms of surveillance quality by considering eight different selected locations and elapsed time. (a) Modified-RMSDCM. (b) Modified-FCP. (c) ISACM. (d) Proposed algorithm.

the charging distance for sensors, forcing them to expend more energy on movement for charging. This reduces the energy available for monitoring tasks, thereby degrading monitoring quality. An excessive number of RS increases the charging cycle duration because the MC must visit each RS to recharge sensors. However, constrained by both the MC's

TABLE III
PERFORMANCE COMPARISON

Algorithm	Maximum	Minimum	Mean
Modified-RMS DCM	0.9056	0.6010	0.7114
Modified-FCP	0.9388	0.7030	0.7940
ISACM	0.9510	0.7500	0.8191
The proposed	0.9956	0.9005	0.9478

limited battery capacity and the data freshness requirement, the charging cycle cannot be extended indefinitely. Consequently, the MC fails to service some sensors before their energy depletion, rendering them incapable of performing monitoring tasks and ultimately degrading the surveillance quality. The P2P3 algorithm fails to account for the random sensor distribution and density imbalance issue. The monitoring quality significantly deteriorates at locations 1, 2, 6, and 7, where sensor deployment is sparser.

The proposed algorithm addresses all three aforementioned issues with corresponding solutions. In the P1 phase, it achieves balanced sensor distribution through attractive-repulsive forces and Voronoi diagrams, significantly improving spatial monitoring quality. In the P2 phase, both the energy constraints of the MC and the working efficiency of sensors are taken into account to optimize the number and placement of RSs. This approach enhances both monitoring quality and charging efficiency. In the P3 phase, the algorithm further improves both spatial and temporal surveillance quality through batch sensor recharging and dynamic monitoring frequency adjustment. Each phase collectively contributes to the overall enhancement of surveillance performance.

Fig. 11 further compares the surveillance quality at eight randomly selected points by applying the proposed algorithm, ISACM, modified-RMSDCM, and modified-FCP. The elapsed time ranges from 0.5 years to 2.5 years. Table III displays the performance comparison among the four algorithms.

The performance range (maximum–minimum difference) analysis reveals that the proposed algorithm achieves the smallest variation ($\Delta = 0.0951$) compared to the three benchmark methods, demonstrating superior stability and consistent performance. This occurs because the sensors in the original scenario follow a random distribution pattern. Specifically, locations 1, 2, 6, and 7 exhibit sparser sensor deployment, while locations 3, 4, and 5 demonstrate denser concentration. The proposed algorithm specifically addresses this uneven distribution characteristic of random sensor deployment. By employing push-pull forces and Voronoi diagram methods, it achieves a more balanced sensor distribution and equilibrates monitoring tasks among sensors, thereby generating more uniform monitoring quality across the entire area. In contrast, the other three algorithms fail to account for the inherent unevenness in random sensor distribution. Consequently, areas with fewer sensors (e.g., locations 1, 2, 6, 7) suffer from degraded monitoring quality, while regions with higher sensor concentration (e.g., locations 3, 4, 5) demonstrate better monitoring performance.

Fig. 12 compares the spatial surveillance quality of the four algorithms. The number of sensors ranges from 400 to 1600, and the elapsed time ranges from 0.5 to 2.5 years. The common trend of the four algorithms is that their spatial surveillance qualities increase with the number of sensors. This occurs because the increasing number of sensors enhance the density of the deployed sensors, thus improving the spatial surveillance quality. In comparison, the proposed algorithm outperforms the existing ISACM, modified-RMSDCM, and modified-FCP. The reasons are stated below. The ISACM algorithm extends the lifetime of WSNs by balancing MC workloads, implementing partial sensor charging, and reducing charger travel costs. However, in the ISACM algorithm, the sensors are randomly distributed across the monitoring area, resulting in uneven density distribution and consequently nonuniform spatial monitoring quality. Areas with lower sensor density exhibit poorer spatial monitoring performance. The modified-RMSDCM algorithm, sensors with low battery levels are unable to perform monitoring tasks while they are being recharged at the recharging center, leading to lower spatial surveillance quality. In the modified-FCP algorithm, sensors in the recharging area assume the role of the MCs. When these sensors are recharging other sensors in the energy transfer zone, they are unable to perform sensing works, resulting in lower surveillance quality in the recharging area, which consequently affects the overall spatial surveillance quality of the region. The proposed algorithm improves the spatial surveillance quality by achieving an even distribution of randomly distributed sensors and employing sensor batch recharging based on recharging intervals.

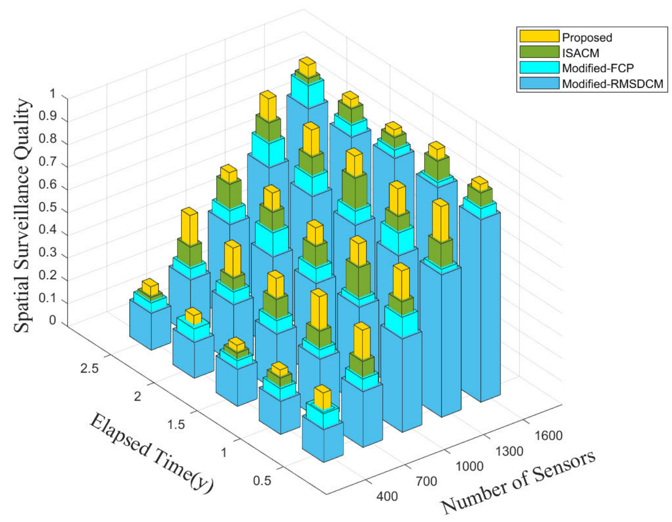

Fig. 12. Comparison of proposed algorithm, ISACM, modified-RMSDCM, and modified-FCP in terms of spatial surveillance quality by considering different numbers of sensors, and elapsed time.

Fig. 13 presents a comparison of the temporal surveillance quality by applying the four compared algorithms. The sensing radius spans from 10 to 30 m. The sensing frequency varies between 1 and 3 times/h. The proposed algorithm is superior to the ISACM, modified-RMSDCM and Modified-FCP algorithms in terms of the temporal surveillance quality. This occurs because the proposed algorithm adjusts the sensor's sensing frequency based on the starting recharging time, aiming to improve temporal monitoring quality. In contrast, the

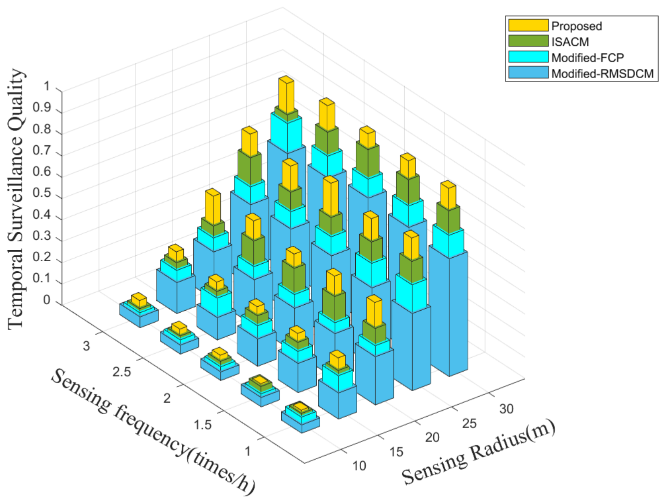

Fig. 13. Comparison of proposed algorithm, ISACM, modified-RMSDCM, and modified-FCP in terms of temporal surveillance quality by considering different sensing radius and frequencies.

ISACM, modified-RMSDCM, and modified-FCP algorithms do not take temporal monitoring quality into account.

VI. Conclusion

This study proposes a cooperative recharging mechanism for WRSNs based on multiple MCs, aiming to maximize surveillance quality while sustaining network lifetime. First, the proposed algorithm effectively addresses the uneven distribution of sensor nodes caused by random deployment through attractive-repulsive forces and Voronoi diagrams, significantly improving the spatial monitoring quality across the surveillance area. Second, the proposed algorithm optimizes both the quantity and placement of RSs while accounting for the energy constraints of MCs, thereby reducing their movement energy consumption. Concurrently, it maximizes the number of sensors simultaneously charged at each RS, significantly improving overall charging efficiency. Finally, the proposed algorithm implements a batch charging strategy to reduce monitoring coverage gap zones during charging cycles, while dynamically adjusting sensor monitoring frequencies based on charging intervals to enhance temporal monitoring quality. The simulation results demonstrate that the proposed cooperative recharging mechanism outperforms the ISACM, modified-RMSDCM and modified-FCP algorithms in terms of energy consumption, charging efficiency, and monitoring quality.

However, some potential limitations and practical challenges remain in this study. The hardware and operational costs associated with multiple MCs may constrain large-scale network deployment, necessitating CE optimization strategies. In addition, sensor nodes need to have mobility and GPS modules, which may increase the complexity of the device. Lightweight or low-power alternatives can be explored in the future. Finally, the current algorithm assumes a relatively stable network topology, whereas real-world obstacles and dynamic interference may compromise charging path planning. Future iterations could integrate reinforcement learning or real-time path optimization techniques to enhance robustness.

References

[1] A. D. Vuong, H. T. Tran, H. N. Q. Pham, Q. M. Bui, T. P. Ngo, and B. T. T. Huynh, "An adaptive charging scheme for large-scale wireless rechargeable sensor networks inspired by deep Q-network," *Neural Comput. Appl.*, vol. 36, no. 17, pp. 10015–10030, Apr. 2024.

[2] A. Naji et al., "ESPP: Efficient sector-based charging scheduling and path planning for WRSNs with hexagonal topology," *IEEE Trans. Sustain. Comput.*, vol. 9, no. 1, pp. 31–45, Jan. 2024.

[3] H. Yu, C.-Y. Chang, W. Guan, Y. Wang, and D. S. Roy, "MC^3: A multicharger cooperative charging mechanism for maximizing surveillance quality in WRSNs," *IEEE Sensors J.*, vol. 24, no. 10, pp. 17080–17091, May 2024.

[4] Z. Wei, M. Li, Z. Wei, L. Cheng, Z. Lyu, and F. Liu, "A novel on-demand charging strategy based on swarm reinforcement learning in WRSNs," *IEEE Access*, vol. 8, pp. 84258–84271, 2020.

[5] A. Kurs, A. Karalis, R. Moffatt, J. D. Joannopoulos, P. Fisher, and M. Soljačić, "Wireless power transfer via strongly coupled magnetic resonances," *Science*, vol. 317, no. 5834, pp. 83–86, Jul. 2007.

[6] J. M. Yi and I. Yoon, "Efficient energy supply using mobile charger for solar-powered wireless sensor networks," *Sensors*, vol. 19, no. 12, pp. 2679–2703, Jun. 2019.

[7] S. He, J. Chen, F. Jiang, D. K. Y. Yau, G. Xing, and Y. Sun, "Energy provisioning in wireless rechargeable sensor networks," *IEEE Trans. Mobile Comput.*, vol. 12, no. 10, pp. 1931–1942, Oct. 2013.

[8] T. Wu, P. Yang, H. Dai, W. Xu, and M. Xu, "Charging oriented sensor placement and flexible scheduling in rechargeable WSNs," in *Proc. IEEE Conf. Comput. Commun.*, Apr. 2019, pp. 73–81.

[9] K. Wang, L. Wang, C. Lin, M. S. Obaidat, and M. Alam, "Prolonging lifetime for wireless rechargeable sensor networks through sleeping and charging scheduling," *Int. J. Commun. Syst.*, vol. 33, no. 8, pp. e4355–e4376, May 2020.

[10] A. Tomar, L. Muduli, and P. K. Jana, "A fuzzy logic-based on-demand charging algorithm for wireless rechargeable sensor networks with multiple chargers," *IEEE Trans. Mobile Comput.*, vol. 20, no. 9, pp. 2715–2727, Sep. 2021.

[11] T. D. Nguyen, T. Nguyen, T. H. Nguyen, K. Nguyen, and P. Le Nguyen, "Joint optimization of charging location and time for network lifetime extension in WRSNs," *IEEE Trans. Green Commun. Netw.*, vol. 6, no. 2, pp. 1186–1197, Jun. 2022.

[12] C. Sha, D. Song, and R. Malekian, "A periodic and distributed energy supplement method based on maximum recharging benefit in sensor networks," *IEEE Internet Things J.*, vol. 8, no. 4, pp. 2649–2669, Feb. 2021.

[13] K. Liu et al., "An active mobile charging and data collection scheme for clustered sensor networks," *IEEE Trans. Veh. Technol.*, vol. 68, no. 5, pp. 5100–5113, May 2019.

[14] Z. Wei et al., "The path planning scheme for joint charging and data collection in WRSNs: A multi-objective optimization method," *J. Netw. Comput. Appl.*, vol. 156, pp. 102565–102577, Apr. 2020.

[15] P. L. Nguyen, V. Q. La, A. D. Nguyen, T. H. Nguyen, and K. Nguyen, "An on-demand charging for connected target coverage in WRSNs using fuzzy logic and Q-learning," *Sensors*, vol. 21, no. 16, pp. 5520–5541, Aug. 2021.

[16] B. Dande, S.-Y. Chen, H.-C. Keh, S.-J. Yang, and D. S. Roy, "Coverage-aware recharging scheduling using mobile charger in wireless sensor networks," *IEEE Access*, vol. 9, pp. 87318–87331, 2021.

[17] C. B. K. Yadav and D. Dash, "An energy efficient periodic data gathering and charging schedule using MVs in wireless rechargeable sensor networks," *Computing*, vol. 105, no. 11, pp. 2563–2593, Nov. 2023.

[18] Y. Dong et al., "Instant on-demand charging strategy with multiple chargers in wireless rechargeable sensor networks," *Ad Hoc Netw.*, vol. 136, pp. 102964–102975, Nov. 2022.

[19] M. U. F. Qaisar, W. Yuan, P. Bellavista, G. Han, and A. Ahmed, "ISAC-assisted wireless rechargeable sensor networks with multiple mobile charging vehicles," *IEEE Internet Things Mag.*, vol. 7, no. 6, pp. 80–86, Nov. 2024.

[20] C.-F. Cheng, C.-C. Wang, and H.-Y. Chang, "An automatic cascaded movement approach to solve the energy replenishment problem in WPT-based mobile WRSNs," *IEEE Trans. Autom. Sci. Eng.*, vol. 21, no. 3, pp. 2763–2778, Jul. 2024.

[21] L.-L. Hung, "Charging protocol for partially rechargeable mobile sensor networks," *Sensors*, vol. 23, no. 7, pp. 3438–3458, Mar. 2023.

[22] G. Wang, G. Cao, and T. F. La Porta, “Movement-assisted sensor deployment,” *IEEE Trans. Mobile Comput.*, vol. 5, no. 6, pp. 640–652, Jun. 2006.

[23] Z. Chen, X. Chen, D. Zhang, and F. Zeng, “Collaborative mobile charging policy for perpetual operation in large-scale wireless rechargeable sensor networks,” *Neurocomputing*, vol. 270, pp. 137–144, Dec. 2017.

Zhijie Hu received the M.S. degree in communication and information systems from Xi’an Technological University, Xi’an, China, in 2011. She is currently pursuing the Ph.D. degree in computer science and technology with Xi’an Jiaotong University, Xi’an.

She is currently a Lecturer at the School of Information Engineering, Xi’an Eurasia University, Xi’an. Her research interests include Internet of Things, wireless sensor networks, and artificial intelligence.

Xiaolin Gui (Member, IEEE) received the B.Sc., M.Sc., and Ph.D. degrees in computer science from Xi’an Jiaotong University, Xi’an, China, 1988, 1993, and 2001, respectively.

He is a Professor at Xi’an Jiaotong University. He has been the Director of the Key Laboratory of Computer Network of Shaanxi Province, China, since 2008. He was in service as the Deputy Dean of the School of Electronic and Information, Xi’an Jiaotong University, from January 2013 to April 2019. He leads the Institute of IoT and Information Security (IoTIS). Since joining XJTU in 1988, he has been an Active Researcher in Network Computing, Network Security, and IoT Application. His recent research covers secure computation of open network systems (include IoT, cloud, and edge computing), federal learning, and privacy protection.

Chih-Yung Chang (Member, IEEE) received the Ph.D. degree in computer science and information engineering from the National Central University, Taoyuan, Taiwan, in 1995.

He is currently a distinguished Professor with the Department of Computer Science and Information Engineering, Tamkang University, New Taipei, Taiwan. His current research interests include artificial intelligence, Internet of Things, wireless sensor networks, and smart healthcare.

Dr. Chang has served as an Associate Guest Editor for several SCI-indexed journals, including *International Journal of Ad Hoc and Ubiquitous Computing* (IJAHUC) from 2011 to 2021, *International Journal of Distributed Sensor Networks* (IJDSN) from 2012 to 2014, *IET Communications* in 2011, *Telecommunication Systems* (TS) in 2010, *Journal of Information Science and Engineering* (JISE) in 2008, and *Journal of Internet Technology* (JIT) from 2004 to 2008.

Xu Zhang received the M.S. degree in electronics and communication engineering from Lanzhou Jiaotong University, Lanzhou, China, in 2009. He is currently pursuing the Ph.D. degree in computer science and technology with Xi’an Jiaotong University, Xi’an, China.

He is currently the Executive Director of Gansu Tongxing Intelligent Technology Development Company Ltd., Lanzhou. His research interests include the digitalization of modern power systems and big data analytics in the field of renewable energy.

Diptendu Sinha Roy received the Ph.D. degree in engineering from the Birla Institute of Technology, Mesra, Ranchi, India, in 2010.

In 2016, he joined the Department of Computer Science and Engineering, National Institute of Technology (NIT) Meghalaya, Shillong, India, as an Associate Professor, where he has been serving as the Chair of the Department of Computer Science and Engineering since January 2017. Prior to his stint at NIT Meghalaya, he had served at the Department of Computer Science and Engineering, National Institute of Science and Technology, Berhampur, India. His current research interests include software reliability, distributed and cloud computing, and IoT, specifically applications of artificial intelligence/machine learning for smart integrated systems.

Dr. Roy is a member of the IEEE Computer Society.